IEEE Robotics and Automation Letters (RA-L) paper, presented at ICRA 2026, Vienna, Austria. Cite as RA-L paper.

Contact Detection and Manipulation With a Shape-Memory Alloy Based Soft Gripper

Louis Plottel, *Graduate Student Member, IEEE*, Richard Desatnik, Dinesh K. Patel, Philip LeDuc, and Carmel Majidi

***Abstract*—Soft robotics offers the opportunity to create dexterous machines that can safely handle delicate objects. Grippers made from deformable actuators and compliant materials can deform around the objects with which they come in contact. The continuum mechanics of flexible manipulators can be leveraged for safe manipulation tasks such as twisting and grasping during manufacturing. However, to achieve this goal, contact sensing and controls for manipulators in these soft systems still remain a challenge in the field. This letter demonstrates a shape-memory alloy actuated soft gripper, with each finger able to bend about multiple axes. This enables the soft gripper to perform twisting tasks and handle various and fragile objects. Using capacitive bend sensors, we also demonstrate that the measured impedance of motion can be used as a proxy for contact, greatly increasing performance in a delicate manipulation task.**

***Index Terms*—Dexterous manipulation, soft robotic applications, soft sensors and actuators.**

I. Introduction

SINCE the turn of the millennium, interest in soft robotic hands has grown significantly due to factors including simplified control, increased robustness to environmental impacts, and improved safety in human-robot interaction [1]. Robotic hands can incorporate soft components in various ways, including rigid hands with compliant padding, hands with deformable joints and rigid links, and hands that are continuously deformable [1], [2]. Continuous deformability, where there is no distinction between joints and links, can offer advantages including enhanced adaptability to the environment and simplified fabrication. Among continuously deformable hands, common actuation methods include fluidic (pneumatic or hydraulic) [2], [3], [4], tendon-based [5], shape-memory material based actuation [6] and stiffness with and without shape memory materials [7], [8]. While fluidic soft grippers are already found in industrial applications [9], [10], they contain drawbacks including weight and bulk due to fluidic control mechanisms such as pumps and valves [11], [12]. Tendon-based actuation contains an analogous drawback in the requirement of motors needed to pull the tendons [12], [13].

Shape memory alloys (SMAs) present an appealing solution for use in robotics because their high power-density and potential for simple actuation can significantly reduce weight and bulk [11], [14], [15]. SMAs are a class of materials that experience a reversible transition between a low-stiffness, low-temperature martensitic phase and a high-stiffness, high-temperature austenitic phase [15], [16]. Further, they possess a "shape-memory" property where they return to a preset geometry when heated above the austenitic transition temperature [15]. Since SMAs are conductive, they can be easily heated via resistive (Joule) heating by applying a current. By embedding shape memory alloys in a deformable structure, roboticists have used the shape memory property of this class of alloys to actuate various robots, including robot hands [6], [12], a brittle star [17], [18], an agile crawler with multistability [19], an amphibious robot [20], and a rhombiferan robot [21]. Despite clear advantages in weight and size, control of SMAs is challenging and is an ongoing area of research [22], [23], [24].

Soft robotic grippers actuated by SMAs have been used predominately in grasping tasks. For example, in [12] the research team built a gripper based on the human middle finger, index finger, and thumb, and in [25] the group demonstrated how an SMA gripper combined with a gecko-inspired contact surface could pick up a variety of objects with different material properties. Another application of SMA grippers has been testing stretchable sensing skin with machine learning to determine contact [26]. In our work we demonstrate the further potential for this form of actuation to be used in twisting tasks based on position information alone.

One promising approach to control of continuously-deformable SMA-actuated robots is closed-loop feedback control. In [27], a capacitive bend sensor was used in conjunction with a simple "bang-bang" controller to oscillate an SMA-powered actuator within a 0.01 cm^{-1} curvature change. [22], [28] use a capacitive bend sensor to monitor the position of continuously-deformable, SMA-actuated robot limbs. In [29], a

Received 23 December 2024; accepted 30 April 2025. Date of publication 6 June 2025; date of current version 17 June 2025. This article was recommended for publication by Associate Editor J. Qu and Editor C. Laschi upon evaluation of the reviewers' comments. This work was supported in part by National GEM Consortium through the GEM Fellows Program (RD) and in part by National Science Foundation (NSF) Human Augmentation via Dexterity Engineering Research Center (HAND ERC). *(Corresponding author: Carmel Majidi.)*

Louis Plottel is with The Robotics Institute, Carnegie Mellon University, Pittsburgh, PA 15213 USA (e-mail: lmplotte@cs.cmu.edu).

Richard Desatnik, Dinesh K. Patel, and Philip LeDuc are with the Department of Mechanical Engineering, Carnegie Mellon University, Pittsburgh, PA 15213 USA (e-mail: rdesatni@andrew.cmu.edu; dineshpa@andrew.cmu.edu; prl@andrew.cmu.edu).

Carmel Majidi is with The Robotics Institute, Carnegie Mellon University, Pittsburgh, PA 15213 USA, and also with the Department of Mechanical Engineering, Carnegie Mellon University, Pittsburgh, PA 15213 USA (e-mail: cmajidi@andrew.cmu.edu).

This article has supplementary downloadable material available at https://doi.org/10.1109/LRA.2025.3577465, provided by the authors.

Digital Object Identifier 10.1109/LRA.2025.3577465

IEEE Robotics and Automation Letters (RA-L) paper, presented at ICRA 2026, Vienna, Austria. Cite as RA-L paper.

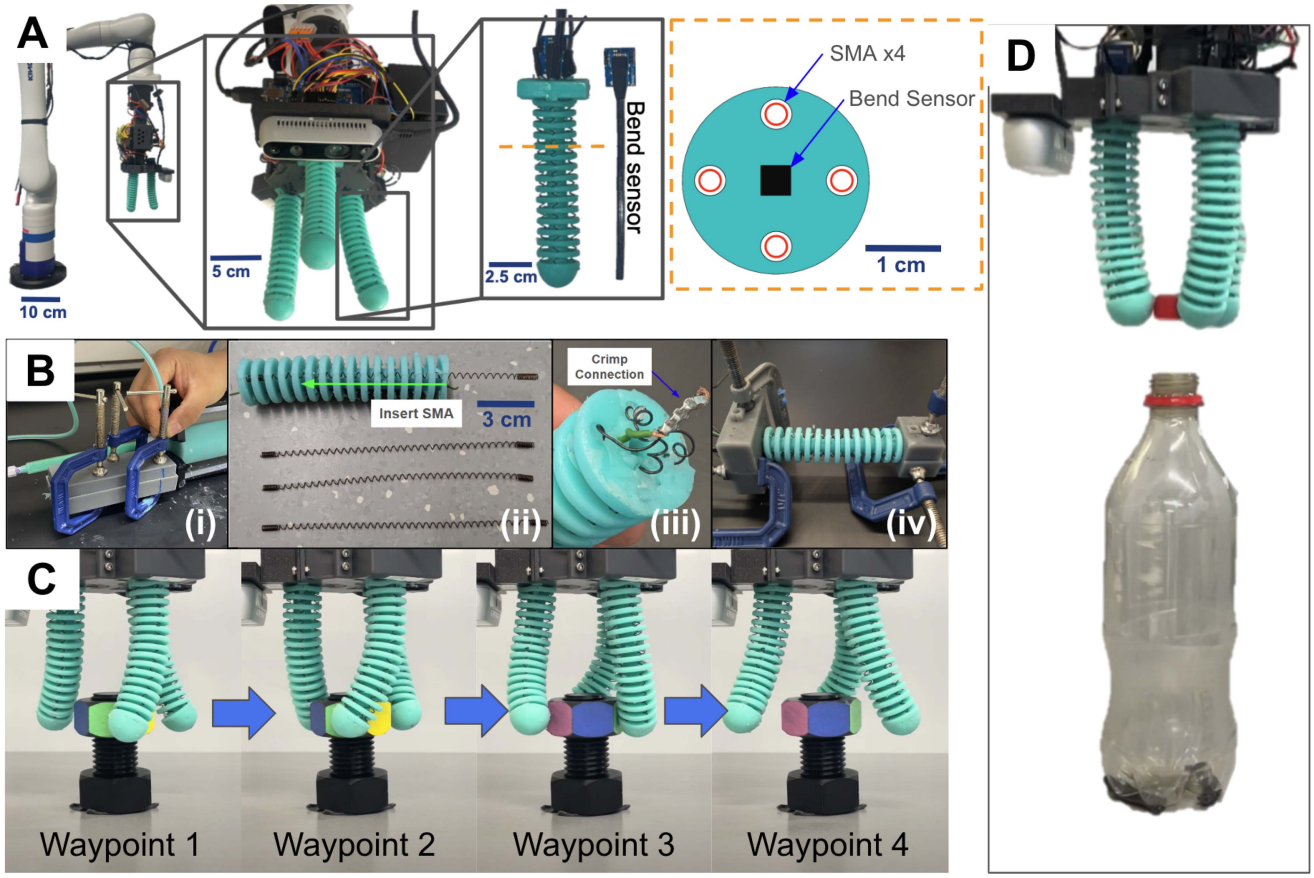

Fig. 1. (a) The hand is mounted to a robotic arm. Each of the three fingers contains four shape-memory alloy (SMA) actuators and one multi-axis bend sensor. (b) Fingers are manufactured by (i) injection molding the finger body, (ii) inserting pre-trained SMA coils, (iii) electrically connecting the SMA coils to a central power line, (iv) molding the base and tip onto the finger (c) A waypoint controller is used to unscrew a nut. (d) A contact detection algorithm is used for fine manipulation tasks such as manipulating a bottle cap.

low-cost hall-effect sensor system is used with a PID controller to successfully follow a trajectory. [30] uses a resistive bend sensor to measure bending in a pneumatically-actuated soft limb. Further, comparison of bending responses under free and constrained movement is used for simple contact detection. In this work, we build on the advancements discussed above in soft robot design, actuation, and sensing to develop a robot hand with the following contributions:

1) A robot hand featuring soft, continuously-deformable fingers actuated by SMAs, capable of bending along multiple axes.
2) Real-time contact detection from pose estimation using capacitive bend sensors embedded within the fingers.
3) Demonstration of complex manipulation tasks including grasping and twisting with simplified control enabled by mechanical compliance and improved manipulation performance through contact detection.

II. Methods

A. Actuator and Sensor Hardware

Each finger in the soft gripper has two pairs of antagonistic SMA actuators, with pairs placed orthogonally to each other. The SMA coil actuators (Flexinol spring, 40 coils, 0.51 mm diameter, Dynalloy Inc.) used in these experiments are composed of Nitinol, an alloy made from around 50% Nickel and 50% Titanium [31]. The SMA coils are pretrained by the manufacturer to contract when heated to a minimal coil pitch. The antagonistic coil placement enables bending about x- and y-axes; as one actuator contracts when heated, the opposing SMA is placed in tension and expands. The SMAs are actuated by Joule heating through a pulse-width modulated (PWM) MOSFET circuit as described in [22]. These circuits are housed in the wrist of the gripper. To handle controlling all 12 SMA actuators, the microcontroller used for the experiments is the Arduino Mega 2560, also housed in the wrist of the gripper. The body of the fingers are made through injection molding using 3D printed molds made on FormLab's resin 3D printer (Fig. 1(b)). The elastomer used in the fingers is Smooth-On's MoldStar 15 SLOW with a 100% modulus of 55psi, a shore hardness of 15 A, and a tensile strength of 400psi [32]. Each finger has a cavity in the middle for a Nitto capacitive bend sensor (2-Axis Soft Flex Sensor, Nitto Bend Technologies) [33]. The sensor measures the angle of the tip relative to the sensor base about two axes. Each finger is attached to the hand with a bracket such that bending in the positive x-direction corresponds to bending toward the

IEEE Robotics and Automation Letters (RA-L) paper, presented at ICRA 2026, Vienna, Austria. Cite as RA-L paper.

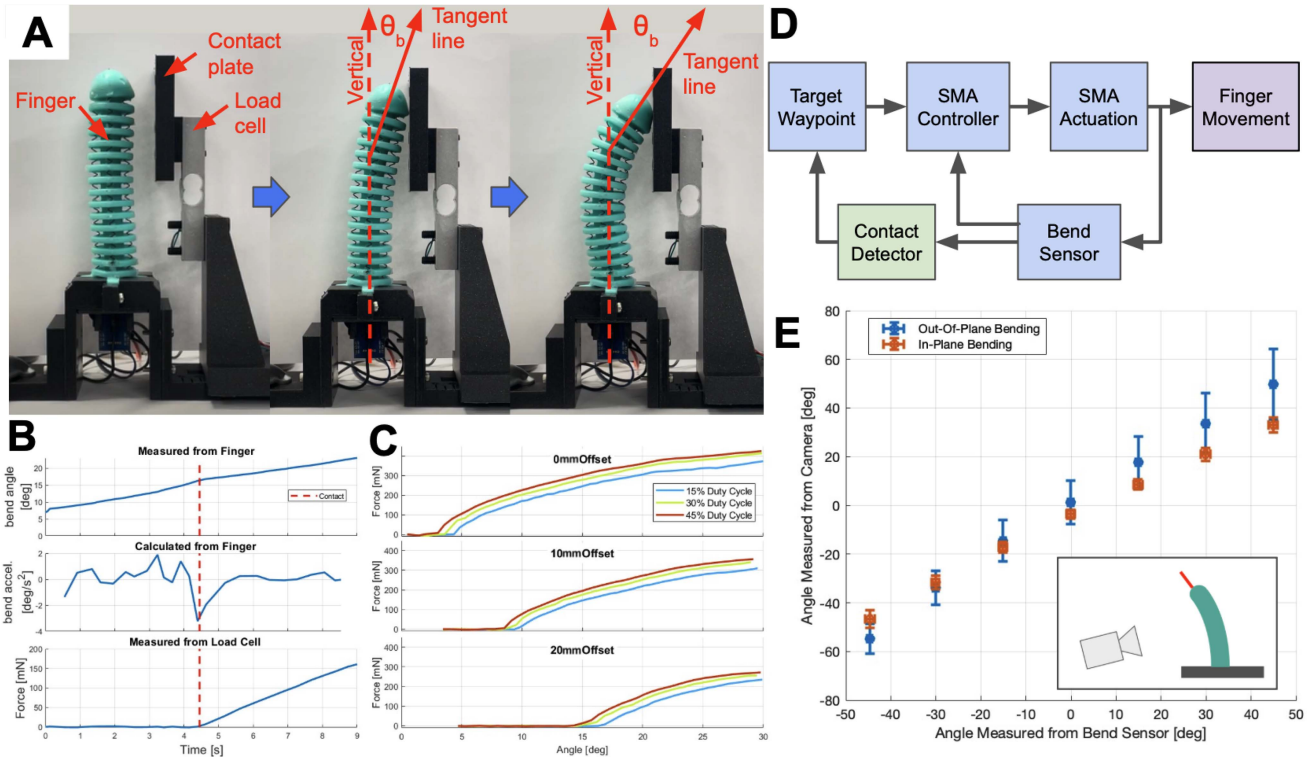

Fig. 2. (a) The testing setup for contact force analysis. One SMA is actuated, causing the finger to bend toward the contact plate. Bend angles and contact force are measured by the integrated bend sensor and a load cell, respectively. The bend angle (θ_b) is measured between a line tangent to the end of the finger and the vertical axis from the base of the sensor (b) A sharp negative acceleration in bend angle occurs at first contact with the contact plate. Test condition for data shown: 20% duty cycle at 7V, 20mm offset. (c) As the finger continues to bend after contact, the measured force increases. Offset distance measures the distance from the contact plate to the closest point on the finger in a neutral (unactuated) position. (d) A feedback control diagram for waypoint control. A contact detector can be optionally added. (e) Experimental comparison of finger angle as measured by the bend sensor and by an external camera. Mean and standard deviations are shown for four fingers.

center of the hand. The configuration of the gripper can be seen in Fig. 1.

B. Finger Characterization

To understand the force relationship from joule heating of each limb, an experiment was conducted to relate the force exerted by the finger to the PWM duty cycle. The experimental setup is shown in Fig. 2(a). The base of the finger is fixed such that the finger is oriented vertically. A load cell is located next to the finger, with a rigidly-attached contact plate positioned at various distances (0 cm, 1 cm, or 2 cm) from the closest point on the finger when the finger is in a neutral (un-actuated) position. The SMA closest to the contact plate is then actuated, causing the finger to bend toward the contact plate. Actuation is performed at a constant duty cycle until 120 seconds has elapsed or the finger reaches a bending angle of 30 degrees as measured by the embedded bend sensor, whichever happens first. The contact force is measured by the load cell. This process is repeated at several duty cycles at 7 Volts, with a 60-second cool-down period in-between actuations. As seen in Fig. 2(b), there is a sharp negative acceleration in the bend angle when contact is made. This insight is used to create a proprioceptive contact detector. Fig. 2(c) shows a graph of contact force over time at 15%, 30% and 45% duty cycles. As the finger continues to bend after contact, the measured force increases. The maximum force measured is about 400 mN.

TABLE I
RESULTS OF CONTACT DETECTION TEST

Cap Diameter	Control Method	Number Correctly Placed	Number Incorrectly Placed
30.5 mm	No Contact Detection	1	9
	Contact Detection	6	4
40.4 mm	No Contact Detection	7	3
	Contact Detection	10	0
45.5 mm	No Contact Detection	1	9
	Contact Detection	9	1

An experiment was performed to test the accuracy of the bend sensors (Fig. 2(e)). A marker was attached to the finger tip and an external camera was used to quantify the accuracy of the bend sensor. Using the waypoint controller, the finger was commanded to spend 30 seconds at seven equally spaced way-points, during which time data was collected. The experiment

TABLE II
COMPARISON OF SMA-ACTUATED HANDS

Finger Count	Finger Length	Max Finger Actuation Force	Max Bending Angle	Bending Response Time	Finger Joints in Plane	Finger Joints Out of Plane	Manipulation Ability	Reference
2	120mm	-	-	-	2	0	**Grasping:** a cardboard box, a plastic cylinder, an orange, a water bottle	[7]
2	∼66mm	∼0.09N	41 degrees	10s	1	0	**Grasping:** a tennis ball, a badminton birdie, a plastic bottle, surgical masks, a table tennis ball, a bolt, a bottle, a pincer, a knife, a cup	[34]
3	100mm	0.89N	400 degrees	1s	1	0	**Grasping:** various fruits and vegetables, sports balls, packaged goods, office supplies, various size bottles and cans, a tumbler, a shoe, toilet paper, a 2kg weight, a stuffed toy	[35]
2	122mm	0.12N	-	-	1	0	**Grasping:** biscuits, a plush teddy bear, a block structure, a yellow duck toy, a balloon, a table tennis ball, a ball structure, a badminton birdie, tape, a candle	[36]
3	120mm	-	∼90 degrees	-	2	0	**Grasping:** a light hollow cylinder, an egg, a red pepper, a frustum	[12]
5	59.4mm-100.78mm	3N (pinch test)	∼180 degrees	-	1	0	**Grasping:** a wire spool, a charger, a table tennis ball, a thin card, a mouse, a tape, a razor, a wire stripper	[6]
3	120mm	0.4N	200 degrees	∼10 deg/sec	1	1	**Grasping:** a bottle, an egg, a chip bag, a ball, bottle caps, **Rotating:** a nut, a bottle cap	**This Work**

was repeated with four fingers. The accuracy was sufficient for effective control implementations as discussed in subsequent sections. Slight discrepancies may be due to sensor slippage within the finger.

C. Contact Detection

As shown in Fig. 2(b), a sharp negative acceleration in bend angle occurs when the finger tip makes contact. The acceleration data shown in Fig. 2(b) is calculated offline. Here, we describe the online implementation of the contact detector. The angular position is sampled using the bend sensor at approximately 18 Hz. To reduce noise and compensate for sensor granularity, the measurements are first passed through a moving-window Gaussian filter ($\sigma = 3, n = 15$). Velocity and acceleration are calculated using a discrete time-difference method. Contact is determined by comparing the finger acceleration to a threshold value. With the finger in an upside-down position and actuated at a 31.4% duty cycle (80/255), an acceleration of less than -8 deg/s^2 was found to indicate contact. This acceleration corresponds to a change in bending rate between free tip movement (pre-contact) and constrained tip movement (during contact). A rules-based approach (e.g., only checking for contact within certain angle bounds) reduces false positives caused by sensor noise and environmental disturbances. While the Gaussian filter introduces a small time delay (less than 1 s with the sampling frequency and filter size mentioned previously), this did not prevent improvements in grasping performance.

D. Waypoint-Based Control

Grasping motions, twisting motions, and mechanical compliance were demonstrated using a simple controller to follow a waypoint-defined path. The methodology is shown in Algorithm 1. The duty cycle for each SMA was set (line 9) using a simple thresholding controller. The duty cycle was set to high with a large error, low with a small error, and zero with a negative error.

This algorithm was evaluated by manipulating several objects. In all cases, the hand was mounted to a Kinova robot arm (see Fig. 1). First, a series of objects were grasped to highlight the abilities of the gripper (Fig. 3(a)–(d)). A Plastic ball is grasped and lifted to demonstrate grasping of a solid object. Subsequently, an unopened foil chip bag is grasped and lifted to show manipulation of a highly deformable object. Then, a plastic bottle and an egg were grasped. Notably, the same control sequence and waypoints are used to grasp the chip bag and the bottle. This demonstrates the ability of a highly compliant gripper to grasp different objects with low software complexity. Finally, in Fig. 1(c) a twisting motion is demonstrated by unscrewing a 3D printed nut from a-3D printed bolt using only finger motions (i.e., stationary wrist).

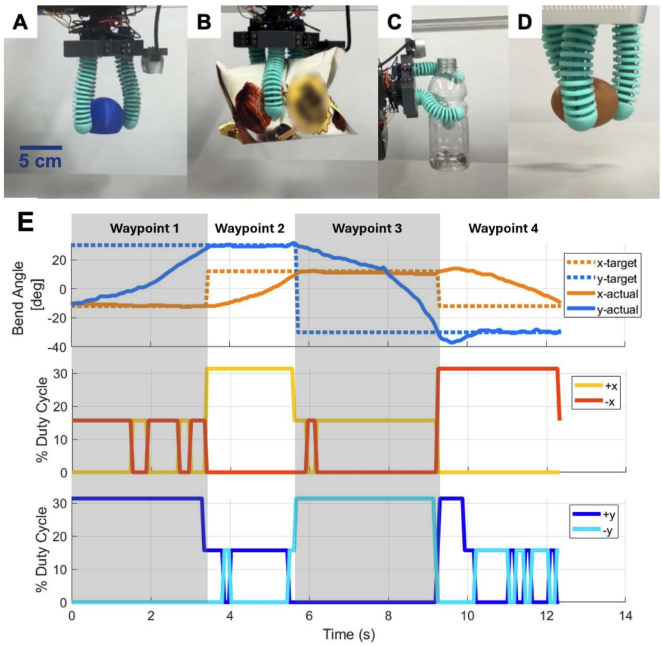

Fig. 3. Grasping (a) a plastic ball, (b) a deformable chip bag (c) a plastic bottle, and (d) an egg. (e) Example data from a waypoint controller. Top: Once a waypoint is reached, the controller progresses to the next waypoint. Middle and bottom: Duty cycles commanded to each SMA to bend the finger to the target waypoints.

Algorithm 1: Waypoint-Based Control.

Require: A sequential list of waypoints for each finger, defined as target angles about finger's x- and y-axes.
Require: Angular position error bound, ϵ.
Initialize the waypoint index to 0.
while waypoint index $<$ `length`(waypoints) **do**
  Measure angular positions of each finger.
  Calculate angular position errors for current waypoint.
  if All angular position errors $\leq \epsilon$ **then**
    Increment waypoint index.
  else
    for each angular position error **do**
      Set duty cycle for the corresponding SMAs.
    end for
    Actuate SMAs at set duty cycles.
  end if
end while

E. Contact Detection Based Control

Contact detection was incorporated into the control sequence (Algorithm 2), and its impact was evaluated using a simple grasping task. The hand was attached to a robot arm as before. Then, bottles with caps of three different diameters (30.5 mm, 40.4 mm, 45.5 mm) were placed below the gripper, with their caps fully loosened. The robot arm moved the gripper to a pre-grasp position above the bottle. The gripper enacted an opened, pre-grasp pose with all fingers at an angle of 30 degrees outward. Fingers then moved to a grasped pose with all fingers at an angle of 15 degrees inward. With contact detection enabled, contact was individually detected for each finger as it moved from the pre-grasp to grasp pose. Once contact was detected, the finger continued to bend to a grasp angle 5 degrees greater than the angle at contact (this increased the force applied to the cap for a better grasp, see Fig. 2(c)). Without contact detection enabled, each finger bent to the grasp angle of 15 degrees. In both cases, the grasp angle was held once reached, and the gripper was raised and lowered, lifting and replacing the cap. The cap was then released. For each cap size, this trial procedure was repeated 10 times with and without contact detection enabled. Other than turning on and off contact detection, no changes were made to the code between trials. The resulting cap position after being placed back on the bottle was categorized as (1) placed correctly (cap is level or near-level), or (2) placed incorrectly (cap is significantly slanted, dropped, placed upside down, or not grasped). Results of this experiment are presented in Table I.

A summary of the experiment is shown in Fig. 4(a)–(b). To quantify the impact of contact detection on applied force, the test setup presented in Fig. 2(a) was used to measure applied force with and without contact detection at distances corresponding to the cap location during grasping. This experiment is summarized in Fig. 4(c)–(e) and was repeated with five different fingers for each condition. Fig. 4(f) shows a final demo in which a bottle cap is grasped, unscrewed, lifted, replaced, and re-tightened, showing the ability of the hand to perform delicate grasping and rotation tasks (Supporting Movie S1).

Algorithm 2: Control Incorporating Contact Detection.

Require: A sequential list of waypoints for each finger, defined as target angles about finger's x- and y-axes.
Require: Angular position error bound, ϵ.
Initialize the waypoint index to 0.
while waypoint index $<$ `length`(waypoints) **do**
  Measure angular positions of each finger.
  Calculate angular position errors for current waypoint.
  Calculate filtered position and derivatives.
  for each finger axis **do**
    if first contact detected {contact detected if accel. $<$ threshold} **then**
      update target angle.
    end if
  end for
  if All angular position errors $\leq \epsilon$ **then**
    Increment waypoint index.
  else
    for each angular position error **do**
      Set duty cycle for the corresponding SMAs.
    end for
    Actuate SMAs at set duty cycles.
  end if
end while

IEEE Robotics and Automation Letters (RA-L) paper, presented at ICRA 2026, Vienna, Austria. Cite as RA-L paper.

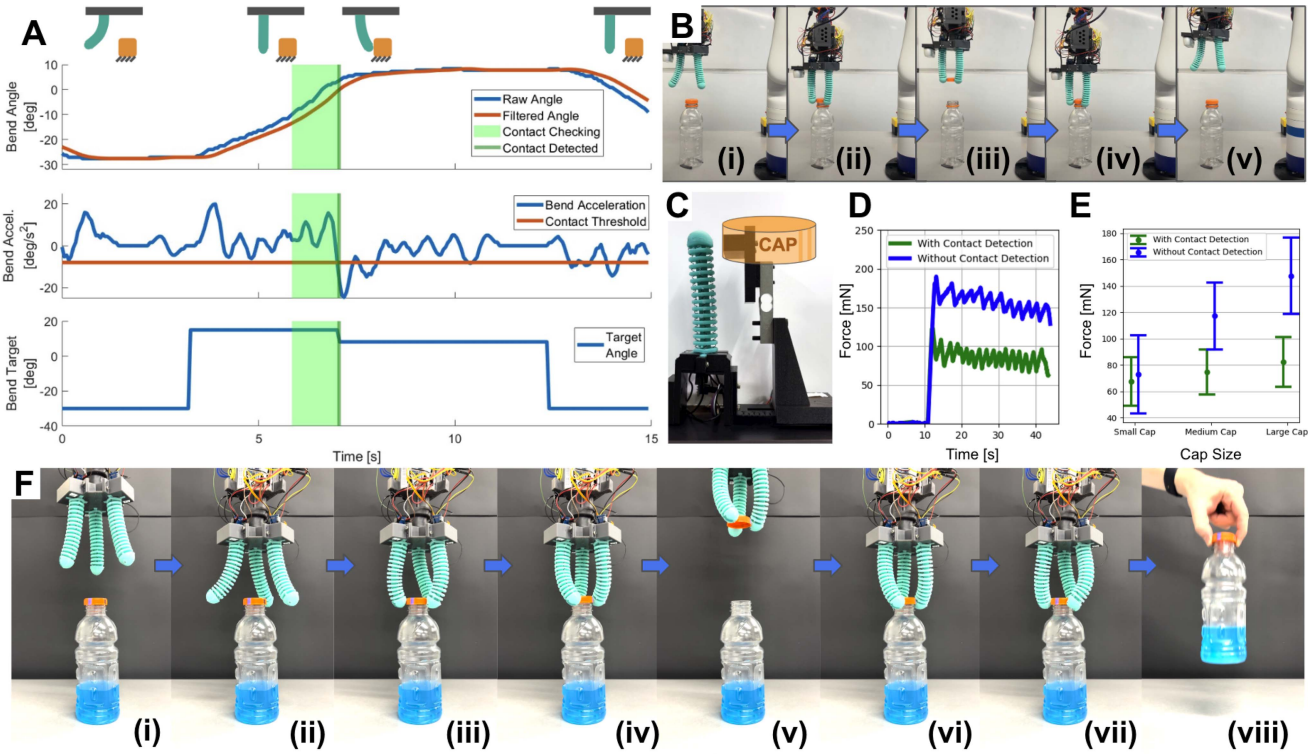

Fig. 4. (a) The finger closes towards a fixed object. When it is near the object, it begins checking the bending acceleration for contact (middle graph). When contact is made, the target bend angle updates (bottom graph). By adjusting the updated target angle after contact, the applied force can be approximately set (Fig. 2(c)). (b) The sequence for testing contact detection. (i) the arm moves to a pre-grasp position and fingers open, (ii) the arm lowers and grasps the bottle cap, (iii) the arm lifts the cap (iv) the bottle cap is replaced (v) the hand lifts up and away. (c) The test setup presented in Fig. 2(a) was used to measure force applied by a finger during grasping with and without contact detection. The contact plate is positioned to correspond to the cap location during grasping. (d) Grasping force over time with and without contact detection at the large cap distance. (e) Five trials were performed for each distance with and without contact detection enabled. Enabling contact detection allows a consistent force to be applied regardless of cap size. (f) A combined demonstration to unscrew, lift, and re-screw a bottle cap: (i) The gripper is positioned above the bottle, (ii) fingers open to a pre-grasp pose, (iii) fingers grasp the cap, (iv) fingers twist to unscrew the cap, (v) the hand lifts the cap, (vi) the hand replaces the cap, (vii) the fingers twist to tighten the cap, (viii) the tightness of the cap is validated by manually lifting the bottle by the cap.

III. Results and Discussion

A. Hand Evaluation

Table II compares our hand with previous SMA-based grippers. Our hand offers significant advantages in manipulation as compared to previous grippers because each finger can bend about two axes along with contact detection. This allows more complex manipulation abilities, such as rotating objects, which includes unscrewing the screw nut and opening the lid of the bottle, along with a variety of grasping tasks.

B. Waypoint-Based Control

The waypoint-based controller was able to successfully grasp different objects, including a plastic ball, a foil chip bag, a bottle, and an egg (Fig. 3(a)–(d)). The controller was also able to demonstrate a twisting motion by unscrewing a 3D-printed bolt. The ability of the hand to grasp the chip bag and the egg with the same control waypoints demonstrates how the compliance of the gripper can accommodate significant differences in grasped objects with a basic controller.

C. Contact Detection Based Control

As shown in Table I, contact detection improved the success rate in the example task of lifting and replacing bottle caps. Of the three bottle caps used, the smallest (30.5 mm diameter) had the overall highest failure rate. The medium cap (40.4 mm diameter) had the highest grasp success rate both with and without contact sensing enabled. The increased diameter may have resulted in greater tolerance for errors in finger placement. Finally, the large cap (45.5 mm diameter) showed good results with contact detection enabled and poor results without contact detection. Since the controller was set to bend fingers inward to an angle of 15 degrees without contact detection, the forces applied by the fingers were larger for the large-diameter cap, which may have contributed to the high failure rate without contact sensing. With contact sensing, the amount of force applied was indirectly controlled by stopping finger movement soon after contact. Fig. 4(e) shows the ability of contact detection to maintain a consistent applied force for all three caps, whereas grasping without contact detection results in significantly higher forces as cap size increases. Additionally, differences in cap texture (knurled vs. smooth) and the interface geometry between the cap and bottle may have influenced success and failure rates among caps.

This experiment shows contact detection can significantly improve the success of a soft gripper in delicate manipulation tasks. By adapting its grasp to each object, a wider array of items can be successfully grasped. More broadly, proprioception, the ability of a robot to sense its internal posture, is a

major challenge for continuously deformable robots. For our continuously deformable fingers, using a multi-axis bend sensor relies on an assumption of constant curvature to estimate finger and tip positions. However, the constant-curvature assumption never holds true in practice due to factors including gravity, air and water currents, and manufacturing defects. Contact sensing offers a means to relax the reliance on the constant-curvature assumption to accomplish useful tasks by allowing relative positions between a finger and grasped object to be updated in real-time upon contact.

IV. Conclusion

We present a new robot hand made of soft, continuously-deformable fingers actuated by shape-memory alloys and embedded with a multi-axis bend sensor to measure finger curvature. We present two control algorithms for this hand. The first, a waypoint-based controller, allows for grasping a range of objects including a ball, a foil bag, a bottle, and an egg. Further, we demonstrate the ability to execute more complex manipulation tasks, including unscrewing a nut. The second controller incorporates contact detection by analyzing the derivatives of curvature measured by the bend sensor. We perform an experiment in which we demonstrate the ability of contact detection to improve task performance by lifting bottle caps of various sizes off of bottles and re-placing them on the bottles. Using contact detection significantly increases the success rate of cap re-placements.

This hand leaves several opportunities for improvement, including refinements to the contact detection algorithm, improvements to finger control through methods such as PID or MPC, and the development of more complex control sequences for even more advanced manipulation tasks. More generally, this study seeks to use SMA as an actuation method due to its intrinsic mechanical compliance and high work and power densities. However, this work does not address some of the weaknesses of using SMA for actuation, including high energy consumption and low cycle rate [37]. This is an open area of research that can potentially be addressed by incorporating active cooling to decrease response times [36] or by modifying the SMA actuator's material composition and crystal structure [14].

Acknowledgment

The authors would like to thank Greg Armstrong and Leonardo Mouta from the JPMorgan Chase & Co. AI Maker Space for access to and assistance with the robot arm.

References

[1] C. Piazza, G. Grioli, M. Catalano, and A. Bicchi, "A century of robotic hands," *Annu. Rev. Control, Robot. Auton. Syst.*, vol. 2, pp. 1–32, 2019. [Online]. Available: https://www.annualreviews.org/content/journals/10.1146/annurev-control-060117-105003

[2] K. Suzumori, S. Iikura, and H. Tanaka, "Development of flexible microactuator and its applications to robotic mechanisms," in *Proc. IEEE Int. Conf. Robot. Automat.*, 1991, vol. 2, pp. 1622–1627.

[3] R. Deimel and O. Brock, "A novel type of compliant and underactuated robotic hand for dexterous grasping," *Int. J. Robot. Res.*, vol. 35, no. 1–3, pp. 161–185, 2016.

[4] D. K. Patel, A. H. Sakhaei, M. Layani, B. Zhang, Q. Ge, and S. Magdassi, "Highly stretchable and UV curable elastomers for digital light processing based 3D printing," *Adv. Mater.*, vol. 29, no. 15, 2017, Art. no. 1606000.

[5] J. P. King et al., "Design. Fabrication, and evaluation of tendon-driven multi-fingered foam hands," in *Proc. IEEE-RAS 18th Int. Conf. Humanoid Robots*, 2018, pp. 1–9.

[6] Y. She, J. Chen, H. Shi, and H.-J. Su, "Modeling and validation of a novel bending actuator for soft robotics applications," *Soft Robot.*, vol. 3, no. 2, pp. 71–81, 2016.

[7] M. Liu, L. Hao, W. Zhang, and Z. Zhao, "A novel design of shape-memory alloy-based soft robotic gripper with variable stiffness," *Int. J. Adv. Robotic Syst.*, vol. 17, no. 1, 2020, Art. no. 1729881420907813.

[8] H. Yang et al., "A compliant metastructure design with reconfigurability up to six degrees of freedom," *Nature Commun.*, vol. 16, no. 1, 2025, Art. no. 719.

[9] L. Birglen, "Enhancing versatility and safety of industrial grippers with adaptive robotic fingers," in *Proc. IEEE/RSJ Int. Conf. Intell. Robots Syst.*, 2015, pp. 2911–2916.

[10] Y. Hao et al., "Universal soft pneumatic robotic gripper with variable effective length," in *Proc. 35th Chin. Control Conf.*, 2016, pp. 6109–6114.

[11] X. Huang, M. Ford, Z. J. Patterson, M. Zarepoor, C. Pan, and C. Majidi, "Shape memory materials for electrically-powered soft machines," *J. Mater. Chem. B*, vol. 8, no. 21, pp. 4539–4551, 2020.

[12] W. Wang and S.-H. Ahn, "Shape memory alloy-based soft gripper with variable stiffness for compliant and effective grasping," *Soft Robot.*, vol. 4, no. 4, pp. 379–389, 2017.

[13] H. Yang et al., "ReCompFig: Designing dynamically reconfigurable kinematic devices using compliant mechanisms and tensioning cables," in *Proc. CHI Conf. Hum. Factors Comput. Syst.*, New York, NY, USA, 2022, pp. 1–4, doi: 10.1145/3491102.3502065.

[14] M.-S. Kim et al., "Shape memory alloy (SMA) actuators: The role of material, form, and scaling effects," *Adv. Mater.*, vol. 35, no. 33, 2023, Art. no. 2208517. [Online]. Available: https://onlinelibrary.wiley.com/doi/abs/10.1002/adma.202208517

[15] S. Stoeckel and J. Simpson, "Actuation and control with shape memory alloys," in *Proc. Conf. Act. Mater. Adaptive Struct.*, 1992, pp. 157–60.

[16] C. Velez et al., "Hierarchical integration of thin-film NiTi actuators using additive manufacturing for microrobotics," *J. Microelectromech. Syst.*, vol. 29, no. 5, pp. 867–873, Oct. 2020.

[17] Z. J. Patterson, A. P. Sabelhaus, K. Chin, T. Hellebrekers, and C. Majidi, "An untethered brittle star-inspired soft robot for closed-loop underwater locomotion," in *Proc. IEEE/RSJ Int. Conf. Intell. Robots Syst.*, 2020, pp. 8758–8764.

[18] Z. J. Patterson, D. K. Patel, S. Bergbreiter, L. Yao, and C. Majidi, "A method for 3D printing and rapid prototyping of fieldable untethered soft robots," *Soft Robot.*, vol. 10, no. 2, pp. 292–300, 2023.

[19] Y. Luo et al., "Intrinsically multistable soft actuator driven by mixed-mode snap-through instabilities," *Adv. Sci.*, vol. 11, no. 18, 2024, Art. no. 2307391. [Online]. Available: https://advanced.onlinelibrary.wiley.com/doi/abs/10.1002/advs.202307391

[20] D. K. Patel et al., "Highly dynamic bistable soft actuator for reconfigurable multimodal soft robots," *Adv. Mater. Technol.*, vol. 8, no. 2, 2023, Art. no. 2201259.

[21] R. Desatnik, Z. J. Patterson, P. Gorzelak, S. Zamora, P. LeDuc, and C. Majidi, "Soft robotics informs how an early echinoderm moved," *Proc. Nat. Acad. Sci.*, vol. 120, no. 46, 2023, Art. no. e2306580120.

[22] R. Desatnik, M. Khrenov, Z. Manchester, P. LeDuc, and C. Majidi, "Optimal control for a shape memory alloy actuated soft digit using iterative learning control," in *Proc. IEEE 7th Int. Conf. Soft Robot.*, 2024, pp. 48–54.

[23] Z. J. Patterson, A. P. Sabelhaus, and C. Majidi, "Robust control of a multi-axis shape memory alloy-driven soft manipulator," *IEEE Robot. Automat. Lett.*, vol. 7, no. 2, pp. 2210–2217, Apr. 2022.

[24] D. J. S. Ruth, J.-W. Sohn, K. Dhanalakshmi, and S.-B. Choi, "Control aspects of shape memory alloys in robotics applications: A review over the last decade," *Sensors*, vol. 22, no. 13, 2022, Art. no. 4860.

[25] M. Modabberifar and M. Spenko, "A shape memory alloy-actuated gecko-inspired robotic gripper," *Sensors Actuators A, Phys.*, vol. 276, pp. 76–82, 2018.

[26] J. Zimmer, T. Hellebrekers, T. Asfour, C. Majidi, and O. Kroemer, "Predicting grasp success with a soft sensing skin and shape-memory actuated gripper," in *Proc. IEEE/RSJ Int. Conf. Intell. Robots Syst.*, 2019, pp. 7120–7127.

[27] Z. Ren, M. Zarepoor, X. Huang, A. P. Sabelhaus, and C. Majidi, "Shape memory alloy (SMA) actuator with embedded liquid metal curvature sensor for closed-loop control," *Front. Robot. AI*, vol. 8, 2021, Art. no. 599650.

[28] A. P. Sabelhaus, Z. J. Patterson, A. T. Wertz, and C. Majidi, "Safe supervisory control of soft robot actuators," *Soft Robot.*, vol. 11, pp. 561–572, 2024.

[29] H. Yang, M. Xu, W. Li, and S. Zhang, "Design and implementation of a soft robotic arm driven by SMA coils," *IEEE Trans. Ind. Electron.*, vol. 66, no. 8, pp. 6108–6116, Aug. 2019.

[30] K. Elgeneidy, G. Neumann, M. Jackson, and N. Lohse, "Directly printable flexible strain sensors for bending and contact feedback of soft actuators," *Front. Robot. AI*, vol. 5, p. 323534, 2018.

[31] Dynalloy Inc., "Technical Characteristics of Flexinol Actuator Wires," Accessed: Jan. 2025. [Online]. Available: https://dynalloy.com/wp-content/uploads/2025/03/TCF1140.pdf

[32] Smooth-On, Mold Star 15. Accessed: Jan. 2025. [Online]. Available: https://www.smooth-on.com/tb/files/MOLD_STAR_15_16_30_TB.pdf

[33] "2-Axis datasheet," NittoBend Technologies, (n.d.). Accessed: Jan. 2025. [Online]. Available: https://www.nitto.com/jp/ja/others/nbt/assets/pdf/two_axis_datasheet.pdf

[34] J. Pan, J. Yu, and X. Pei, "A novel shape memory alloy actuated soft gripper imitated hand behavior," *Front. Mech. Eng.*, vol. 17, no. 4, 2022, Art. no. 44.

[35] J.-H. Lee, Y. S. Chung, and H. Rodrigue, "Long shape memory alloy tendon-based soft robotic actuators and implementation as a soft gripper," *Sci. Reports*, vol. 9, no. 1, 2019, Art. no. 11251.

[36] X. Li et al., "A fast actuated soft gripper based on shape memory alloy wires," *Smart Mater. Structures*, vol. 33, no. 4, 2024, Art. no. 045011.

[37] S. I. Rich, R. J. Wood, and C. Majidi, "Untethered soft robotics," *Nature Electron.*, vol. 1, no. 2, pp. 102–112, 2018.